Model-Based Adaptive Prognosis of a Hydraulic System

Sawan Kumar, Sumanta Kumar Dutta, Sanjoy Kumar Ghoshal and J. Das

Abstract Fault diagnostic and prognostic methods are the extensive topics of condition-based maintenance system. These publications include a wide range of statistical approaches for model-based approaches. Uncertainty in prediction cannot be avoided; therefore, algorithms are working to help manage these uncertainties. Remaining useful lives (RUL) are regularly updated through adaptive degradation models identified by using the concept of sampling importance resampling (SIR) filter. The SIR filter algorithm has become a popular choice for model-based progressive system. As a matter of study, we consider a hydraulic system and develop a detailed physics-based model and use extensive simulations to describe our prehistoric science approach and to evaluate its effectiveness and strength.

Keywords Hydraulic system · RUL · SIR filter

1 Introduction

Energy crisis and destabilization of fuel prices have accelerated the research on the fuel-efficient system. Model-based diagnostics approach is required for precise and infallible models of actual physical systems which incorporate several domains (such as mechanical, electrical and hydraulic). Behavior can be non-ambiguous, and it may be challenging to capture the connection between individual components and between the system and their environment.

Apart from this, different systems used in the real world are multi-models, i.e., operations are carried out in various configurations. An important challenge is modeling the system's mobility in a serious and effective way. In practice, the major challenge is balancing the details amalgamated into the model to ensure diagnosability, while keeping the complication in the model within controllable

S. Kumar (✉) · S. K. Dutta · S. K. Ghoshal
Department of Mechanical Engineering, IIT(ISM) Dhanbad, Dhanbad, India
e-mail: nawaskumar@gmail.com

J. Das
Department of Mining Machinery Engineering, IIT(ISM) Dhanbad, Dhanbad, India

H. Kumar and P. K. Jain (eds.), *Recent Advances in Mechanical Engineering*,
Lecture Notes in Mechanical Engineering,
https://doi.org/10.1007/978-981-15-1071-7_32

limits. Wu et al. [1] have discussed various types of energy saving techniques. The overall system efficiency depends upon the robustness of the system, which is only achievable with proper fault detection of the system. This is also related to the energy regeneration purpose [2]. Detecting faults (when something goes wrong), fault isolation (determining the fault location), identification of fault (determining fault mode) and prognostics (depending on the expected nature of continuous use, the occurrence of failure is predicted) are the sequential steps of complete fault diagnosis. Determination of fault detection and isolation (FDI) with a quantitative approach necessitates the generation of a mathematical model of the system. Use of the different constraints and different compatibility conditions has been presented in terms of known variables using the residual relations which are termed as analytical redundancy relations (ARRs) [3]. According to the normal operation of the model, the constraints are valid. The adaptive thresholds have been generated from the residual relations with small deviations of the constraints that are taken into account for the observation of the normal mode of operation. The number of sensors is proportional to the structured residuals. This is used for the fault detection and isolation purpose. Unstructured residual allows estimating the time-dependent behavior of the process parameters, which can be used for fault detection by comparison with the nominal values. Using the ARRs, the fault signature matrix (FSM) can be formed which is responsible for the identification of the faulty components. The unexpected deviations in the parameters of the system are termed as faults. Then, as faults transpire and stimulate the deviation of measurements, the observed deviations in measurements are compared to predicted values for the given particular faults, and any fault causing inconsistency when compared to the observed measurement deviations is removed from consideration [4]. The prediction for the end of the system's life is made by using a predictor on the basis of a mistake progress model integrated with nominal models for each hypothesized fault candidate. Many diagnostics and prognosis are used on the simulation model of the hydraulic system and the results are presented.

	Fault detection	Prognostics	Diagnostics
Machine learning	Clustering	Neural network	Decision trees
Physics-based	System theory	Damage propagation models	
Conventional numerical	Linear regression	Kalman filters	Logistic regression
AI-model-based	Expert systems		Finite-state machines

The paper structure is as follows. Section 2 accommodates the details of the behavioral and diagnostic model of the system. Section 3 explains in detail the method of diagnosis and prognosis used in this work. Section 4 includes experimental results and Sect. 5 provides a reasonable conclusion for the paper.

2 Modeling of the Hydraulic System

2.1 Model-Based Approaches

For the implementation of a model-based progressive approach, the components require a detailed physics-based model. Nominal behavior, as well as defective behavior of the component, should be described by the model. Apart from this, the progress of fault should be defined over time. It is with these models that can be predicted. Developing a nominal model based on the physical understanding of the system is the initial step in the way of developing models that meet the previously described requirements.

2.2 Physical Description of the System

The schematic representation of the setup being studied is shown in Fig. 1. Table 1 gives the names of the different components of the setup corresponding to the tags given in Fig. 1. The setup has a double-acting variable displacement pump (tag 2), driven by a 7.5 kW electric motor (tag 1), furnishing pressurized fluid to a bent axis hydromotor (tag 6). Before reaching the hydromotor, the fluid passes through a proportional flow control valve (tag 4), which is operated using a solenoid, which modulates the flow supplied to the hydromotor corresponding to the voltage imparted to the flow control valve. The hydromotor is used to drive a single-acting fixed displacement loading pump (tag 7) which in turn supplies fluid to the reservoir (tag 12.1–12.4) through a pressure relief valve (PRV) (tag 9). The load torque of the motor is regulated by varying the pressure setting of the PRV. The experiments are

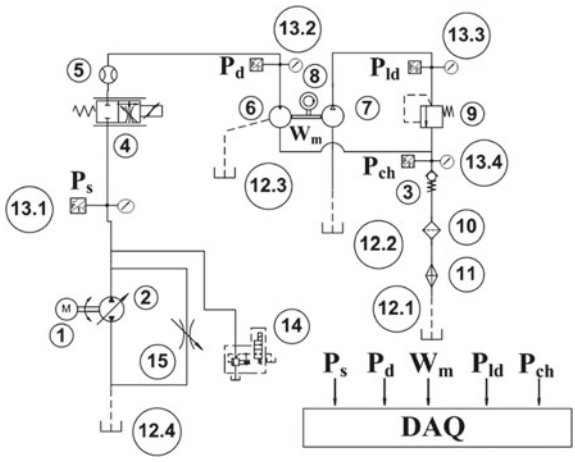

Fig. 1 Schematic representation of the setup

Table 1 The different components in the schematic diagram

Tag No.	Name of equipment
1	Electrical drive motor
2	Variable displacement pump
3	Spring-loaded check valve
4	Proportional flow control valve
5	Flow sensor
6	Motor
7	Loading pump (fixed displacement)
8	Speed sensor
9	Pressure relief valve
10	Filter
11	Oil cooler
12.1–12.4	Hydraulic reservoir
13.1–13.4	Pressure sensor
14	Flow control valve
15	Flow restrictor valve

conducted on the setup under well-aerated conditions. To obtain fluid with constant viscosity at different parts of the setup, suitable oil cooler and filter are used. The oil cooler maintains the temperature of the fluid in the range of 55–62 °C. The experimental setup has four pressure sensors (tag 13.1–13.4) and a speed sensor (tag 8) to measure the pressure at different sections of the system and the speed of the driven hydromotor which is recorded in the data acquisition system (DAQ). To ensure the accuracy of the setup, multiple test runs are conducted before collecting the data.

2.3 Mathematical Modeling of the System

The assumptions made for the mathematical modeling of the system are as follows:

- The fluid used in the system is a Newtonian fluid.
- The rate of flow through the flow control valve has a nonlinear relationship with the pressure difference across it.
- Details of valve dynamics assimilating spool inertia and friction effects are not taken into consideration.
- Compression of the fluid during flow through pipes is not considered.

2.3.1 Variable Displacement Pump

The volume flow rate lost due to compression in the pump can be mathematically given as

$$Q_p = D_p\omega_p - \frac{P_s}{L_p} - \left(C_D A\sqrt{\frac{2(|P_s - P_d|)}{\rho}}\mathrm{Sgn}(P_s - P_d)\right) \tag{1}$$

where

Q_p = Volume flow rate provided by the pump
D_p = Variable pump displacement
L_p = Resistance to leakage in variable displacement pump
D_s = Main pump pressure or system pressure
C_D = Coefficient of discharge
A = Orifice area of the proportional valve
P_d = Proportional relief valve pressure or delivery pressure = $k_{\text{bulk}} \int Q_m \mathrm{d}t$
$P_s = k_{\text{bulk}} \int Q_p \mathrm{d}t$, k_{bulk} = bulk modulus.

2.3.2 Hydraulic Motor

The volume flow rate lost due to compression in the hydraulic motor can be mathematically given as

$$Q_m = \left(C_D A\sqrt{\frac{2(|P_s - P_d|)}{\rho}}\mathrm{Sgn}(P_s - P_d)\right) - D_m\omega_m - \frac{P_d}{L_m} \tag{2}$$

where

Q_m = Volume flow rate lost due to compression in the hydraulic motor
D_m = Volumetric displacement of hydraulic motor
L_m = Resistance to leakage in hydraulic motor
ω_m = Angular velocity of hydraulic motor.

Now, torque lost in the motor to overcome rotational inertia is

$$T_m = D_m(P_d - P_{ch}) - f\omega_m - D_{lp}P_{ld} \tag{3}$$

where

P_{ch} = Check valve pressure at loading circuit
f = Viscous friction coefficient
D_{lp} = Loading pump displacement

P_{ld} = Discharge pressure of the loading pump.
$\omega_m = \frac{\int T_m \mathrm{d}t}{\text{Motor Inertia}} = \frac{\int T_m \mathrm{d}t}{J}$

Now, flow to the tank from the motor can be described as

$$Q_{m1} = D_m\omega_m - \left(C_d A_{\text{ch}}\sqrt{\frac{2(|P_{\text{ch}} - P_{\text{atm}}|)}{\rho}}\text{sgn}(P_{\text{ch}} - P_{\text{atm}})\right) + \left(C_d A_l\sqrt{\frac{2(|P_{\text{ld}} - P_{\text{ch}}|)}{\rho}}\text{sgn}(P_{\text{ld}} - P_{\text{ch}})\right) \tag{4}$$

And corresponding effort = $P_{\text{ch}} = k_{\text{bulk}}\int Q_{m1}\mathrm{d}t$
where

A_{ch} = Orifice area of the check valve at load circuit
P_{atm} = Atmospheric pressure.

2.3.3 Loading Pump

Loading pump which is coupled with the hydraulic motor also experiences some hydraulic losses during fluid flowing through the pump. Now, the flow from the pump is given as,

$$Q_{\text{lp}} = D_{\text{lp}}\omega_m - \left(C_d A_l\sqrt{\frac{2(|P_{\text{ld}} - P_{\text{ch}}|)}{\rho}}\text{sgn}(P_{\text{ld}} - P_{\text{ch}})\right) \tag{5}$$

where the pressure at the inlet to the loading pump = $P_{\text{ld}} = k_{\text{bulk}}\int Q_{\text{lp}}\mathrm{d}t$

A_l = Orifice area of the load valve.

2.3.4 Residuals

In this application, five sensors are used, and therefore, the number of residuals will be five.

From Eq. (1), the first residual can be described as below:

$$\text{Rd}_1 = D_p\omega_p - \frac{\dot{P}_s}{k_{\text{bulk}}} - \left(\frac{P_s}{L_p}\right) - \left(C_D A\sqrt{\frac{2(|P_s - P_d|)}{\rho}}\text{Sgn}(P_s - P_d)\right) \tag{6}$$

and

$$\varepsilon_1 = \frac{|\dot{P}_s|}{\delta k_{\text{blk}}} + \left(\delta D_p |\omega_p|\right) + [\delta(C_D A)]\sqrt{\frac{2|P_s - P_d|}{\rho}} + \frac{|P_s|}{\delta L_p}$$

where δ is the uncertainty for the associated parameter and its value is considered as 0.1 (i.e., 10%).

Upper threshold value $= \text{Rd}_1 + \varepsilon_1$
Lower threshold value $= Rd_1 - \varepsilon_1$

The second residual corresponding to the second equation is

$$\text{Rd}_2 = \left(C_D A\sqrt{\frac{2(|P_s - P_d|)}{\rho}}\text{Sgn}(P_s - P_d)\right) - D_m\omega_m - \frac{\dot{P}_d}{k_{\text{bulk}}} - \frac{P_d}{L_m} \tag{7}$$

and

$$\varepsilon_2 = \frac{|\dot{P}_d|}{\delta k_{\text{blk}}} + (\delta D_m|\omega_m|) + [\delta(C_D A)]\sqrt{\frac{2|P_s - P_d|}{\rho}} + \frac{|P_d|}{L_m}$$

Upper threshold value $= \text{Rd}_2 + \varepsilon_2$
Lower threshold value $= \text{Rd}_2 - \varepsilon_2$

According to Eq. (3), the third residual is as follows:

$$\text{Rd}_3 = D_m(P_d - P_{\text{ch}}) - f\omega_m - D_{\text{lp}}P_{\text{ld}} - J\dot{\omega}_m \tag{8}$$

and

$$\varepsilon_3 = \delta D_m|P_d - P_{\text{ch}}| + (\delta f|\omega_m|) + \left(\delta D_{\text{lp}}|P_{\text{ld}}|\right) + (\delta J|\dot{\omega}_m|)$$

Upper threshold value $= \text{Rd}_3 + \varepsilon_3$
Lower threshold value $= \text{Rd}_3 - \varepsilon_3$

From Eq. (5), the fourth residual can be described as below:

$$\text{Rd}_4 = \frac{\dot{P}_{\text{ld}}}{k_{\text{blk}}} - D_{\text{lp}}\omega_m + C_D A_l\sqrt{\frac{2|P_{\text{ld}} - P_{\text{ch}}|}{\rho}}\text{sgn}(P_{\text{ld}} - P_{\text{ch}}) \tag{9}$$

and

$$\varepsilon_4 = \frac{|\dot{P}_{\text{ld}}|}{\delta k_{\text{blk}}} + \left(\delta D_{lp}|\omega_m|\right) + [\delta(C_D A_l)]\sqrt{\frac{2|P_{\text{ld}} - P_{\text{ch}}|}{\rho}}$$

Upper threshold value $= \mathrm{Rd}_4 + \varepsilon_4$
Lower threshold value $= \mathrm{Rd}_4 - \varepsilon_4$

From Eq. (4), the fifth residual can be described as

$$\mathrm{Rd}_5 = D_m\omega_m - \left(C_d A_{\mathrm{ch}}\sqrt{\frac{2(|P_{\mathrm{ch}} - P_{\mathrm{atm}}|)}{\rho}}\mathrm{sgn}(P_{\mathrm{ch}} - P_{\mathrm{atm}})\right) + \left(C_d A_l\sqrt{\frac{2(|P_{\mathrm{ld}} - P_{\mathrm{ch}}|)}{\rho}}\mathrm{sgn}(P_{\mathrm{ld}} - P_{\mathrm{ch}})\right) - \frac{\dot{P}_{\mathrm{ch}}}{k_{\mathrm{bulk}}} \tag{10}$$

and

$$\varepsilon_5 = (\delta D_m|\omega_m|) + \left(\delta(C_d A_{\mathrm{ch}})\sqrt{\frac{2(|P_{\mathrm{ch}} - P_{\mathrm{atm}}|)}{\rho}}\right) + \left(\delta(C_d A_l)\sqrt{\frac{2(|P_{\mathrm{ld}} - P_{\mathrm{ch}}|)}{\rho}}\right) + \frac{|\dot{P}_{\mathrm{ch}}|}{\delta k_{\mathrm{bulk}}}$$

Upper threshold value $= \mathrm{Rd}_5 + \varepsilon_5$
Lower threshold value $= \mathrm{Rd}_5 - \varepsilon_5$

From the five residual equations from Eqs. (6) to (10), the fault signature matrix is derived in Table 2, which correlates the components with their fault likelihood.

2.4 Simulink Model of the System

According to the mathematical equations of the above section, a block model is made in MATLAB/Simulink. The model has been divided into two parts—behavioral model and diagnostic model (Fig. 2). In the behavioral model, the constitutive relations given in Eqs. (1) through (5) are evaluated, whereas the diagnostic model is a simple computation of the residuals given in Eqs. (6) through (10).

3 Adaptive Prognosis Approach

3.1 Degradation Model and RUL Prediction

System input, $u(k)$, measurement, $t(0{:}\ k)$, and the initial state of the system are taken as input of small model supervisor, and state transition function, $f(k)$ and observation function, $h(k)$, state distribution, $y(k)$, and parameter, $\theta(k)$ is used to estimate $p(y(k),$

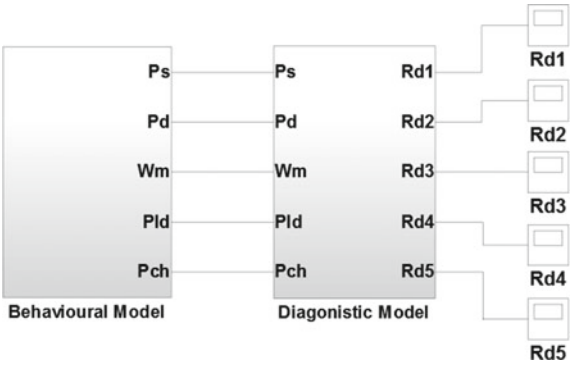

Fig. 2 Simulink model of the system

$z(k) \mid t(0{:}\,k)$. Any suitable filtering scheme, e.g., Kalman filter, extended Kalman filter, unscented Kalman filter, particle filter, SIR filter [5] and others, can be appointed as the nominal observer. According to the fault signature matrix (FSM), the probable components can be identified during the breakdown of the machine for a particular type problem. But there are some faults which cannot be isolated because of its nature. In the given FSM, if only the first residual (Rd_1) deviates, then it is not isolable between V_p and L_p. The reason is that fault signature is same, i.e., coherence vector $C^{'}$= [1 0 0 0 0] for V_p and L_p.

3.2 Proposed Prognosis Procedure

3.2.1 Damage Estimation

In the model-based paradigm, estimation of the loss reduces joint states-parameter estimation, i.e., calculation of $f(\boldsymbol{y}_k, z_k, |z_{0:k})$. For linear systems with additive Gaussian noise terms, the particle filter serves as the most appropriate option [6]. For nonlinear systems with additive Gaussian noise terms, the unscented Kalman filter or extended Kalman filter also works as suitable alternatives [7]. However, for nonlinear systems with non-Gaussian noise conditions, particle filters are most suitable and provide accurate (i.e., sub-adoption) solutions to the state calculation problem for those systems where the optimum solution is unrecoverable or unmanageable. In particle filters, a set of discrete weighted specimens called particle helps to estimate, almost accurate, state distribution. As the number of particles grows, increasing accuracy ensures that optimal solution stops. In addition, implementation of particle filters is relatively straightforward, and increasing or decreasing the number of particles controls the computational complexity, with respect to the preferred estimation performance. Furthermore, other filtering algorithms are unable to directly handle the discrete position sensors. For these reasons, our model-based prognostics framework utilizes sampling importance resampling (SIR) particle filters. With particle

filters, the particle approximation to the state distribution is given by

$$\left\{\left(\boldsymbol{y}_k^i, \boldsymbol{z}_k^i\right), \omega_k^i\right\}_{i=1}^N$$

where N denotes the number of particles, and for particle, i.e., $\boldsymbol{y}_k^i$ parameter shows the estimates, $\boldsymbol{z}_k^i$ denotes the parameter estimates and ω_k^i denotes the weight.

The posterior density is estimated by

$$f(\boldsymbol{y}_k, \boldsymbol{z}_k, |\boldsymbol{z}_{0:k}) \approx \sum_{i=1}^{N} \omega_k^i \delta_{\left(\boldsymbol{y}_k^i, \boldsymbol{z}_k^i\right)}(\mathrm{d}t_k \mathrm{d}z_k)$$

where $\delta_{\left(\boldsymbol{y}_k^i, \boldsymbol{z}_k^i\right)}(\mathrm{d}t_k \mathrm{d}z_k)$ denotes the Dirac delta function located at $(\boldsymbol{y}_k^i, \boldsymbol{z}_k^i)$.

The sample importance reproduction (SIR) employs particle filters, and by using systematic reproduction, the resampling phase is applied. The pseudo-code for single phase of SIR filter is shown as Algorithm 1 [8]. Each particle i is propagated periodically by sample of new parameter values. Here, the parameter $\boldsymbol{z}_k$ is developed by some unknown random process which is independent of the state $\boldsymbol{y}_k$. To assess the parameters within a SIR filter structure, however, we need to assign parameters to some type of development. Specific solutions are to use a random walk, i.e., for parameter $\boldsymbol{z}$, $\boldsymbol{z}_k = \boldsymbol{z}_{k-1} + \xi_{k-1}$ where ξ_{k-1} is typically Gaussian noise. After sampling parameter values from selected distribution, new states are taken sampling by implementing state equation f to $(\boldsymbol{y}_k^i, \boldsymbol{z}_k^i)$ with process noise $v(t)$ sampled from its assumed distribution. The particle weight is assigned using z_k. Specifically, the output equation h is applied to $(\boldsymbol{y}_{k+1}^i : \boldsymbol{z}_{k+1}^i)$ and the probability of this output is calculated using the probability of sensor noise using the probability density function. Weight is then normalized, followed by resampling step [9]. Therefore, within the algorithm, we believe that some sensor noise exists for these sensors.

3.2.2 Prediction

Prediction is started at a certain time t_p. Using the current state estimate, $f(\boldsymbol{y}_k, \boldsymbol{z}_k, |\boldsymbol{z}_{0:k})$ the goal is to compute $f(\mathrm{EOL}_{t_p}, |\boldsymbol{z}_{0:t_p})$ and $f(\mathrm{RUL}_{t_p}, |\boldsymbol{z}_{0:t_p})$. The particle filter computes

$$f\left(\mathrm{EOL}_{t_p} | \boldsymbol{z}_{0:t_p}\right) \approx \sum_{i=1}^{N} \omega_{t_p}^i \delta_{\left(\mathrm{EOL}_{t_p}^i\right)}\left(\mathrm{dEOL}_{t_p}\right).$$

To calculate EOL, we proliferate each particle ahead of its specific EOL and weigh the particle on t_p compute EOL, for its EOL prediction.

4 Results and Discussions

In our experiments, to find fault, we use the nominal system simulation model to produce the behavior of the nominal system. In our experiments and the parameters of the hydraulic system, fault signatures for defects are given in Table 2, and errors are used for isolation. For identifying the fault, we use sampling importance resampling (SIR) as its supervisor. Parameter is updated through the given weight to the EOL and RUL and gives the appropriate result.

4.1 System Identification and Experimentally Validation

Figure 3a through Fig. 3d compare the measured and simulated pressure at different points in the circuit for the purpose of fault diagnosis. The parameter values (given in Table 3) obtained from the product catalogue of the set-up are used for model simulation. In Fig. 3, experimental pressure is slightly more than the simulation pressure. The nature of curve is almost similar after adjusting some parameter. The

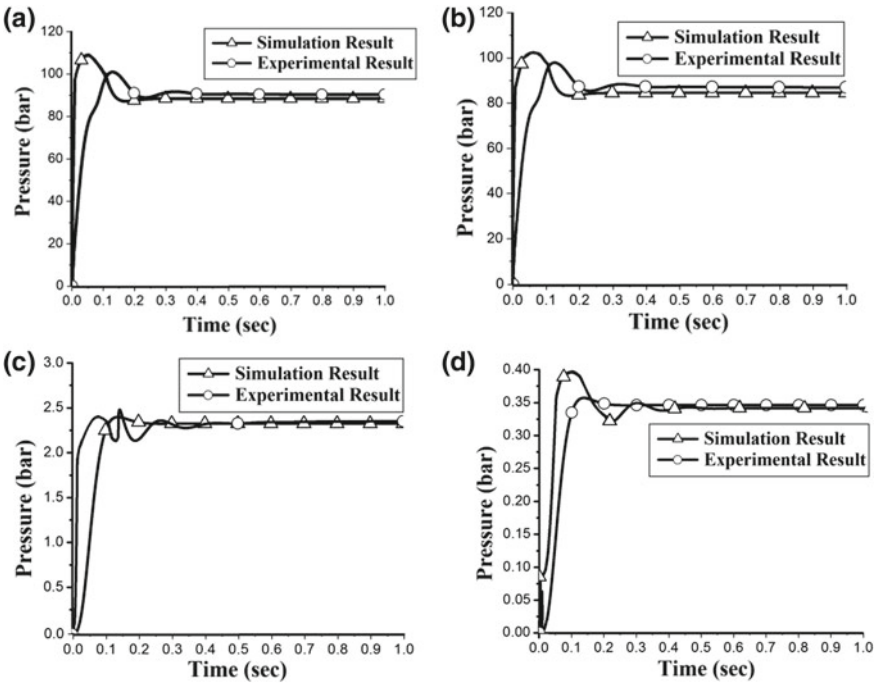

Fig. 3 **a** System pressure (E_s) versus time. **b** Delivery pressure (E_d) versus time. **c** Loading pressure (E_{ld}) versus time. **d** Check valve (E_{ch}) pressure versus time

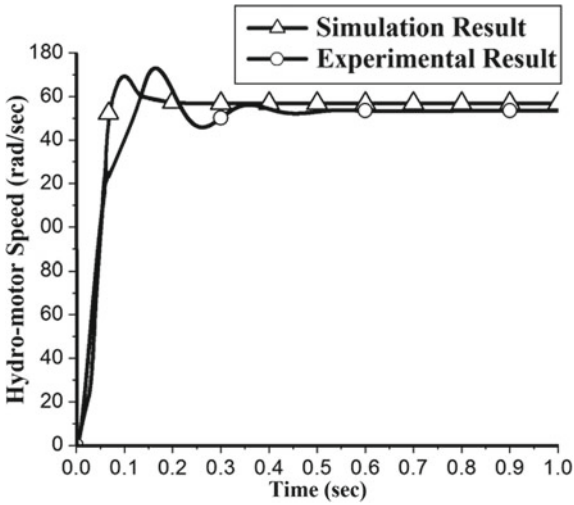

Fig. 4 Motor speed (ω_m) versus time

peak time is shifted in experimental behavior. The reason is that in the model simulations different nonlinearities caused by flow-force, pump ripples, etc. are not considered, while experimental analysis involves all such factors. Apart from that errors due to measurement and process noise are also reflected in the test data.

In Fig. 4, the experimental rotational speed of hydromotor is slightly less than simulation result. It is due to the viscous friction of the revolving component, which is not identified in the model.

4.2 Residual Evaluation Using Test Data

Two types of faults are imposed one after another. First one is the reduction of pump displacement (i.e., Vp reduced) and the next is the reduction of the leakage resistance across the variable displacement pump (i.e., Lp reduced) at 5 s. Only Rd_1 is crossing the threshold as shown in Figs. 5 and 6, respectively. Only Rd_1 is deflected beyond the range of the threshold. Now, the task is to isolate the faulty component through parameter estimation.

4.3 Demonstration of the Approach

The behavior received by the model supports the model-based approach in contrast to simple trending strategies. To demonstrate a general solution, the particle filter is permitted to estimate all the damage modes of the hydraulic system jointly. Taking into consideration the large state space, $T = 40000$ s is implemented. For each fault

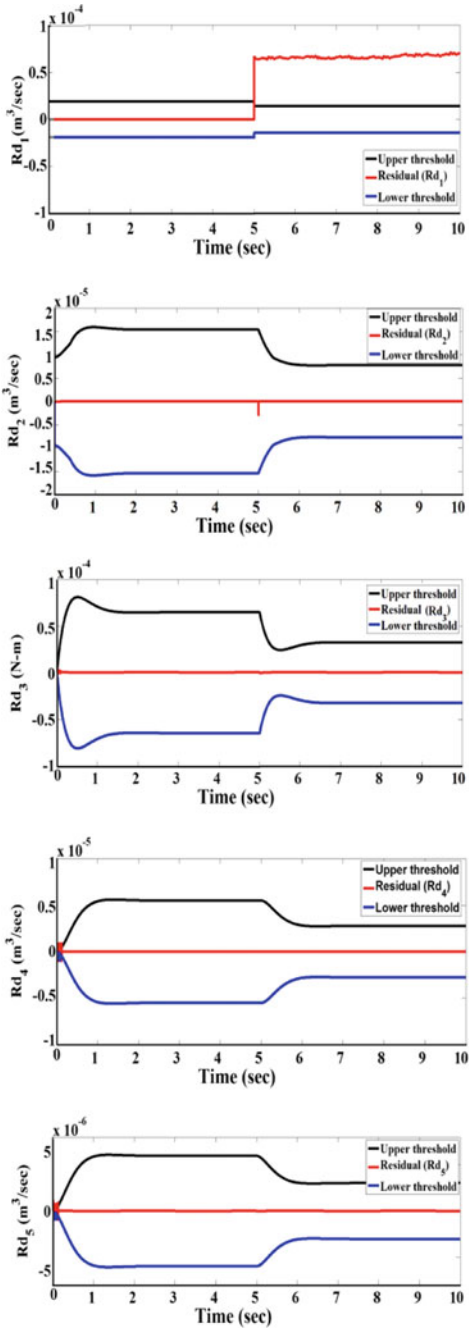

Fig. 5 Upper threshold, residual and lower threshold versus time after imposing the fault in the displacement of pump

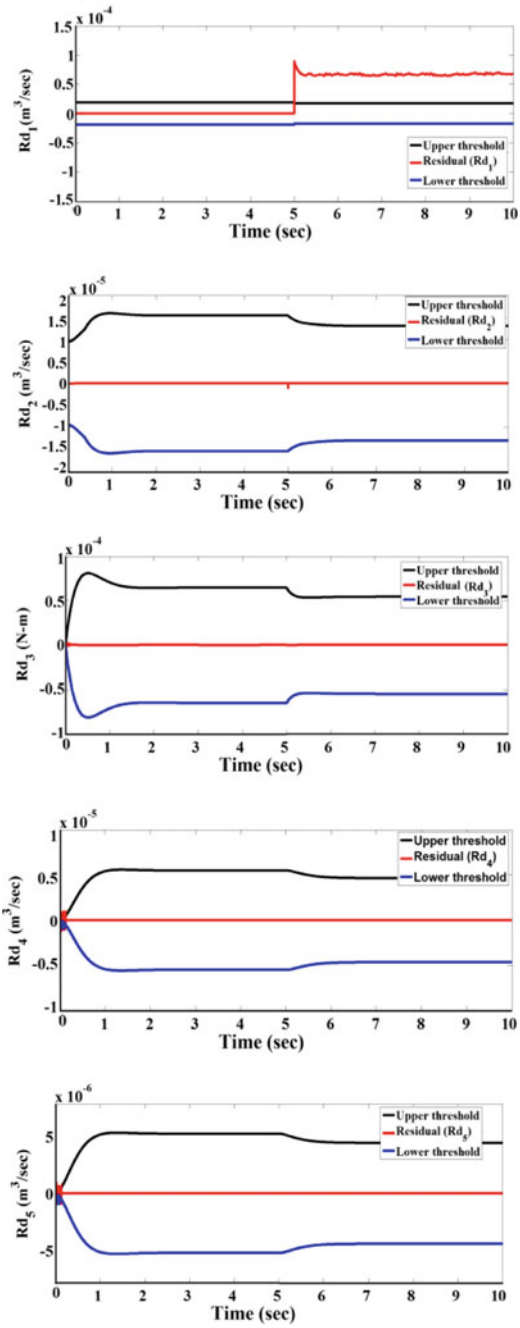

Fig. 6 Upper threshold, residual and lower threshold versus time after imposing the fault in the leakage of pump

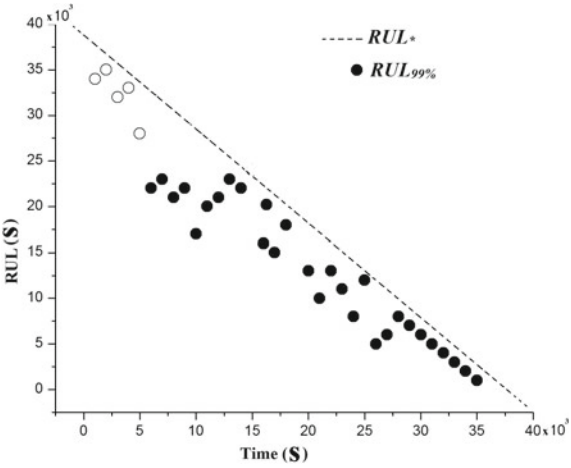

Fig. 7 RUL*(true) versus $RUL_{99\%}$

mode, the proposed algorithm provides the correct wear rate. The identified fault in this particular study is the external leakage from pump-plenum. Figure 7 captures the 99% confidence-level predictions, i.e., the value at which 99% of the prediction distribution is greater than or equal to that value. At this level of confidence, the predictions always remain below the true RUL and work as conservative estimates, and decisions can be taken on the basis of these risks. For more complete verification, a more flexible test is required, such that it may be run to fail the defect and/or the injection of hydraulic system.

For this, the estimated value of displacement of the pump (Dp) is obtained as 2.839×10^{-6} m^3/rad and leakage resistance (L_p) is 1.5×10^{11} N s/m^2, whereas the nominal values for D_p and L_p are 3.14×10^{-6} m^3/rad and 1×10^{11} N s/m^2, respectively (refer Tables 2 and 3). But the increase of leakage above the nominal is not admissible. Hence, the admissible solution is the reduction of pump displacement to 2.839×10^{-6} m^3/rad.

Table 2 Fault signature matrix

Components	Rd_1	Rd_2	Rd_3	Rd_4	Rd_5	I
D_p	1	0	0	0	0	0
D_m	0	1	1	0	1	1
A	1	1	0	0	0	1
A_l	0	0	0	1	1	1
D_{lp}	0	0	1	1	0	1
L_p	1	0	0	0	0	0
L_m	0	1	0	0	0	1
f	0	0	1	0	0	1

Table 3 Parameters of components used in Simulation

Parameters	Value
Electric motor speed (ω_p)	150 rad/s
Fixed pump displacement (D_p)	3.15×10^{-6} m^3/rad
Bulk stiffness (k_{bulk})	5×10^{12} N/m^2
Resistance to pump leakage flow path (L_p)	1×10^{11} N s/m^2
Coefficient of discharge (C_D)	0.64
Density of the fluid (ρ)	865.7 m^3/kg
Proportional leakage area (A)	2×10^{-5} m^2
Motor displacement (D_m)	1.91×10^{-6} m^3/rad
Inertia of motor (J)	0.01 kg m^2
Motor leakage (L_m)	1×10^{12} N s/m^2
Loading pump displacement (D_{lp})	1.75×10^{-6} m^3/rad
Proportional leakage area constant for loading circuit (A_l)	2×10^{-5} m^2
Proportional leakage area constant for motor (A_{ch})	1×10^{-4} m^2
Atmospheric pressure (P_{atm})	1×10^5 Pa
Viscous friction (f)	0.1 N s/m^2

5 Conclusions

In the course of this work, a model-based prognostics system approach making the use of SIR filters for updated parameter estimation has been developed. The estimated damage of the hydraulic system predicted EOL and forms EOL and RUL distributions. Applying this method to a hydraulic system, we develop an exhaustive physics-based model that includes models of damage progression. From the simulated experiments, it can be established that using only the discrete position sensors of the hydraulic system, successful prognostics can be achieved, and this approach is applied to experimental data under the same constraint. The effectiveness of a model-based approach is demonstrated by the results, and insight into the parameters considered for the selection of sensors for valve prognostics is given. A model-based approach is advocated, where the performance depends greatly upon the accuracy of the model provided. Undoubtedly, a key obstacle is presented in the development of such a model.

Acknowledgements I am grateful to DST project number YSS/2015/000397 "Design and development of series-parallel hydraulic hybrid energy efficient excavator having displacement con-trolled actuators" for providing the setup for doing future research in this field.

References

1. Wu W, Hu J, Jing C, Jiang Z, Yuan S (2014) Investigation of energy efficient hydraulic hybrid propulsion system for automobiles. Energy 73:497–505
2. Lin T, Huang W, Ren H, Fu S, Liu Q (2016) New compound energy regeneration system and control strategy for hybrid hydraulic excavators. Autom Constr 68:11–20
3. Shi H, Yang H, Gong G, Liu H, Hou D (2014) Energy saving of cutterhead hydraulic drive system of shield tunneling machine. Autom Constr 37:11–21
4. Kumar S, Das S, Ghoshal SK, Das J (2018) Review of different energy saving strategies applicable to hydraulic hybrid systems used in heavy vehicles. IOP Conf Ser Mater Sci Eng 377(1):012072. (IOP Publishing)
5. Roychoudhury I, Hafiychuk V, Goebel K (2013) Model-based diagnosis and prognosis of a water recycling system. In: Aerospace conference, IEEE, pp 1–9
6. Mahulkar V, McGinnis H, Derriso M, Adams DE (2010) Fault identification in an electro-hydraulic actuator and experimental validation of prognosis based life extending control. Air force research lab wright-patterson AFB OH air vehicles directorate
7. Prakash O, Samantaray AK, Bhattacharyya R, Ghoshal SK (2018) Adaptive prognosis for a multi-component dynamical system of unknown degradation modes. IFAC-PapersOnLine 51(24):184–191
8. Pandian A, Ali A (2009) A review of recent trends in machine diagnosis and prognosis algorithms. In: 2009 world congress on nature and biologically inspired computing. NaBIC 2009, IEEE, pp 1731–1736
9. Daigle MJ, Goebel K (2011) A model-based prognostics approach applied to pneumatic valves. Int J Progn Health Manag 2(2):84–99